

On a Simple Method of Obtaining Sidelobe Reduction over a Wide Angular Range in One and Two Dimensions

Ronald J. Pogorzelski
Jet Propulsion Laboratory
California Institute of Technology
Pasadena, CA 91109-8099

Abstract

A patented technique for suppressing the sidelobes of an array antenna is considered. This technique involves the addition of two elements, one at each end of the array, which together produce an interferometer pattern used for cancellation of sidelobes. It is shown here that the technique is most effective for uniform illumination and that there then exists an optimum fixed position for the added elements. The amplitude of the excitation of the auxiliary elements determines the angular location of the region of sidelobe reduction while the phase of the excitation tracks the beam-steering phase of the array. Thus, this technique is seen to be easily implemented in an array controlled by coupled oscillators. The technique generalizes in a straightforward manner to two-dimensional arrays in which case a set of auxiliary elements on the perimeter of the array is required. A two dimensional oscillator controlled array of this type is described here with which one can produce a main beam and a sidelobe suppression region which can be independently positioned anywhere in a hemisphere provided they do not coincide.

I. Introduction.

In many communications and radar applications, one is confronted with interfering signals originating in a predefined angular sector. In such a case, one would like to design the antenna to be insensitive to signals in that angular sector while maintaining high sensitivity in the direction of its main beam. Depending on the particular situation, one may desire that either or both the main beam and the suppressed angular sector be steerable. In treating this design problem, we consider initially the simple case of a one-dimensional linear array of $2N+1$ discrete radiating elements as represented in Figure 1. This case was treated in a Patent Disclosure by Michael A. Kott in which he described a method for sidelobe cancellation involving the use of an auxiliary interferometer consisting of two elements added to the array, one at each end as in Figure 2.[1] While the separation between the end elements of the original array and the added elements was not specified by Kott, he did suggest that a possible separation might be equal to the inter-element spacing of the original array. Kott showed by example that, for typical aperture taper, one could adjust the relative phase of the excitation of the added elements about a nominal 180 degrees to bring the interferometer lobes of the added elements into alignment with the sidelobes of the original array pattern in the vicinity of a specified angular position in the far zone. Then, by subtraction of the interferometer pattern from

that of the original array with proper amplitude weighting, one could cancel the sidelobes in the vicinity of that angular position. This nearly eliminated the sidelobe in question while significantly reducing neighboring sidelobes as well thus producing a wide-angle suppression of the antenna sensitivity. Finally, Kott also pointed out that several such arrays could be placed side by side to produce a horizontal fan beam with reduced sidelobes around a specified elevation angle or a vertical fan beam with reduced sensitivity around a specified azimuth angle.

Prior to Kott's work, Tseng discussed the design of Taylor weighted arrays and apertures having far zone patterns with a specified angular region of reduced sensitivity.[2] He achieved the desired pattern by adjusting the positions of the zeros of the array factor placing them closer together in the suppression region and further apart elsewhere. In doing this he noted that such suppression required modification of the aperture distribution only near the ends of the array. This is, of course, consistent with the method of Kott in which the aperture distribution is augmented at the ends of the array.

Recently, Liao and York introduced a method of beam-steering applicable to linear arrays using an array of coupled electronic oscillators to produce the necessary element excitations.[3] They showed that the beam of such an array could be electronically steered without the use of phase shifters by controlling the free running frequencies of the end oscillators of the oscillator array. Pogorzelski, et al. [4] provided a convenient linearized theory describing the dynamic behavior of such arrays and Pogorzelski [5] generalized the analysis to the analogous two dimensional array wherein the steering is accomplished by controlling the free running frequencies of the perimeter oscillators, a great simplification over the conventional beam-steering control system using phase shifters. Inherent in these concepts, however, is the assumption of uniform oscillator amplitude throughout the array. While various aperture tapers could be obtained by adjusting the gains of the amplifiers between each oscillator and its corresponding radiating element, the most natural taper resulting from this arrangement is the uniform taper. Thus, it is of interest to investigate the implications of uniform aperture illumination when applying Kott's sidelobe suppression scheme to oscillator controlled arrays. As will be shown here, the uniform taper is, in a mathematical sense, the ideal taper for Kott's scheme and, in fact, the coupled oscillator system provides a means of achieving optimum results under the uniform aperture illumination assumption. Extending Kott's work, it is further shown that the entire concept is quite naturally generalized to a two dimensional array with a steerable pencil beam thus providing a suppression region which is independently steerable to any desired position outside the main beam regardless of the beam-steering angle.

II. A Linear Array with Uniform Illumination.

For simplicity in describing the concept, the elements will be treated as scalar isotropic radiators. Element pattern and polarization effects are easily accounted for in the case of

a practical design. In terms of the inter-element spacing, s , which is assumed to uniform across the array, the far zone radiation field is given by,

$$E(\theta) = \sum_{n=-M}^M A_n e^{-jmk s u(\theta)} \quad (1)$$

where

$$u(\theta) = \sin \theta - \sin \theta_B$$

and A_n is the amplitude of the excitation of the n th element, k is the wavenumber, θ is the angular position of the field point, and θ_B is the angular position of the beam peak. Again for simplicity of presentation, we suppose that the excitation is uniform across the array; i.e., $A_n=1$. In that case, the expression for E can be summed in closed form. The result is,

$$E(\theta) = \frac{\sin[(M + \frac{1}{2})ksu(\theta)]}{\sin[\frac{1}{2}ksu(\theta)]} \quad (2)$$

A. Sidelobe Suppression

Following Kott, consider the case where two elements are added to the array, one at each end, such that they are separated from the original end elements by a distance d as shown in Figure 2. Let the amplitude of their excitation be P and let the phase of their excitation be p . Let a subscript “-” denote the element added at position $-Ns+d$ and let a subscript “+” denote the element added at position $Ns+d$. The total field radiated by the augmented array can be written,

$$E_T(\theta) = \frac{\sin[(M + \frac{1}{2})ksu(\theta)]}{\sin[\frac{1}{2}ksu(\theta)]} + P_- e^{jp_-} e^{jk(Ms+d)\sin \theta} + P_+ e^{jp_+} e^{-jk(Ms+d)\sin \theta} \quad (3)$$

We wish to set the values of P and p for each added element so as to achieve the objective of a sector of reduced gain centered at a specified angle, θ_s . The approach is to set the phase, p , so that the lobes of the interference pattern of the two added elements are matched in width to the sidelobes of the original array and then to set the amplitudes, P , to cancel the sidelobes of the original array in the desired angular region. We proceed as follows.

First, since the first term of (3) is real, the second and third terms will have to be complex conjugates. Thus, $p_+ = -p_- = p$ and $P_- = P_+ = P$. Equation (3) then becomes,

$$E_T(\theta) = \frac{\sin[(M + \frac{1}{2})ksu(\theta)]}{\sin[\frac{1}{2}ksu(\theta)]} + 2P \cos[k(Ms + d)\sin\theta - p] \quad (4)$$

Next, we choose $d = \frac{s}{2}$ and $p = -\frac{\pi}{2} + (M + \frac{1}{2})ks \sin\theta_B$ resulting in,

$$E_T(\theta) = \frac{\sin[(M + \frac{1}{2})ksu(\theta)]}{\sin[\frac{1}{2}ksu(\theta)]} - 2P \sin[(M + \frac{1}{2})ks(\sin\theta - \sin\theta_B)] \quad (5)$$

It is now quite obvious that the desired goal can be achieved by properly setting the value of P; that is, setting

$$P = \frac{1}{2 \sin[\frac{1}{2}ks(\sin\theta_s - \sin\theta_B)]} = \frac{1}{2 \sin[\frac{1}{2}ksu(\theta_s)]} \quad (6)$$

results in a total field,

$$E_T(\theta) = \frac{\sin[(M + \frac{1}{2})ksu(\theta)]}{\sin[\frac{1}{2}ksu(\theta)]} - \frac{\sin[(M + \frac{1}{2})ksu(\theta)]}{\sin[\frac{1}{2}ksu(\theta_s)]} \quad (7)$$

which obviously has a zero at $\theta = \theta_s$. More importantly, however, it has a small magnitude in a wide region surrounding $\theta = \theta_s$ by virtue of the matching of the lobe widths discussed above. In fact, in this respect it may be more informative to rewrite (7) in the form,

$$E_T(\theta) = \left\{ \csc[\frac{1}{2}ksu(\theta)] - \csc[\frac{1}{2}ksu(\theta_s)] \right\} \left\{ \sin[(M + \frac{1}{2})ksu(\theta)] \right\} \quad (8)$$

Here the first factor in curly brackets gives the envelope of the sidelobes while the second factor contains the rapid variation. Thus, the region of sidelobe suppression extends over the range for which the first factor remains small.

B. Numerical Examples

To illustrate the effectiveness of the technique described above, we compute a number of simple examples and plot the far zone gain of the array. That is, we plot

$$G(\theta) = 20 \log_{10} \left(\frac{|E(\theta)|}{\sqrt{2M+1}} \right) \quad (9)$$

The array to be considered is a 21-element array ($M=10$) with half wavelength spacing. The two added elements are then spaced one-quarter wavelength from the end elements. We begin with the case of an unscanned beam and select the suppression region to be centered at 30 degrees from broadside. The resulting pattern is shown in Figure 3a together with the pattern of the original array without the added elements. Note that the suppression extends over several sidelobes. Note also that, because the pattern of the added elements is antisymmetric, the sidelobes for negative angles are enhanced. This result is to be compared with the traditional nulling technique using a single added element weighted to place a null at 30 degrees. The result is shown in Figure 3b and exhibits a much narrower suppression region.

Next, consider an array with the main beam steered to -30 degrees from broadside and apply sidelobe suppression centered at 30 degrees as before. The result is shown in Figure 4. Here the suppression is even more effective due to the greater angle between the main lobe and the suppression region. This implies that if the suppression region were chosen close to the main lobe, the suppression would be reduced in effectiveness. This is verified in the case plotted in Figure 5 where the main lobe is unscanned but the suppression region is centered at 8 degrees. Here sidelobes for both positive and negative angles are enhanced and the suppression region is much narrower. Thus, the suppression is less effective near the main lobe and more effective far from the main lobe. The transition between these two extremes can be taken to occur when no sidelobes on the same side of the main beam as the suppression region are increased in level. From (8) it can be shown that this occurs at,

$$\csc\left[\frac{1}{2}ksu(\theta_s)\right] = 2 \quad (10)$$

which for the present case reduces to,

$$\sin \theta_s - \sin \theta_B = \frac{1}{3} \quad (11)$$

This transition case is illustrated in Figure 6 where the main beam is scanned to -30 degrees while, according to (11), the suppression region is centered at -9.594 degrees. As anticipated, none of the sidelobes to the right of the main beam are increased.

C. Discussion of the Linear Array.

Kott's sidelobe suppression scheme has been applied here to a linear array with uniform illumination. It has been shown that if the separation of the added elements from the end elements of the array is set to exactly half the inter-element separation of the original array and if the phases of the added elements are set to a value which is linearly extrapolated from the phases of the original array elements and augmented appropriately by ± 90 degrees, the zeros of the pattern of the added elements exactly coincide with the zeros of the original array pattern. This will only be true for uniform illumination. It is in this sense that the uniform case is the ideal one for the Kott suppression scheme; that is, it yields the widest possible suppression region. For any other taper, the interferometer pattern must be adjusted to match the zeros where suppression is desired and will not match the zeros elsewhere in the pattern of the original array. For example, Kott suggested that the added elements might be placed one inter-element spacing away from the end elements of the original array. If this is done and the phase, p , is adjusted to produce cancellation of the pattern at the desired suppression angle; that is,

$$p = -\frac{\pi}{2} + (M+1)ks \sin \theta_B - \frac{1}{2}ksu(\theta_S) \quad (12)$$

a somewhat degraded suppression centered at θ_S is obtained. As a specific example, consider the case shown in Figure 3 in which the beam is unscanned and the suppression is centered at 30 degrees. Figure 7 shows the result of using (12) superimposed on the patterns of Figure 3. Note that the width of the suppression region is reduced. However, the impact on the rest of the pattern is also reduced resulting in a lesser increase in sidelobe level than that resulting from the optimum element spacing. Of course, for any but uniform aperture illumination, one is left no choice but to adjust p for best alignment of the lobes for cancellation as described and spacing of the added elements is of lesser importance.

Recalling Tseng's work [2], one might at this point wonder why the necessary modification of the aperture distribution to achieve sidelobe suppression was found to lie not at the ends of the array but, rather, somewhat inside the aperture. After all, in the analysis above, placing the added elements at half the inter-element spacing from the end elements of the original array can be viewed as placing them at the outer edge of the last unit cell of the original array; i.e., at the aperture edge. The explanation is, of course, that Tseng's sidelobe suppression is symmetrical. That is, he creates a notch in the sidelobes on both sides of the beam whereas Kott's notch exists on only one side. Thus, the interferometer lobes of the added elements, which would normally have a null at the angle of the main beam, must be adjusted so as to slip one half cycle with respect to the sidelobes of the original array as one passes from one suppression region to the one on the opposite side of the main beam. This is accomplished by reducing the spacing of the added elements thus widening their interferometer lobes a bit. In fact, this places the added elements within the aperture of the original array. Further evidence of this can be found in Tseng's Figure 5. wherein it is shown that suppression closer to the main beam

requires more extreme narrowing of the interferometer aperture; i.e. more extreme widening of the lobes, to achieve the phase reversal in the corresponding shorter angular range between suppression regions.

Returning to the oscillator controlled array, in light of the above results, the system shown in Figure 8 is proposed and shown to possess several desirable features. The oscillators are assumed to be voltage controlled. That is, voltages applied to their tuning ports determine their free running frequencies. First, note that the phase difference between oscillators is limited to 90 degrees in order that the oscillators remain mutually injection locked as described by Liao and York. Thus, for half wavelength spacing of the radiating elements, if every oscillator is connected to a radiating element, the achievable beam-steering range is limited to plus and minus 30 degrees from boresight. However, if only every other oscillator is connected to a radiating element, this range extends to endfire. This arrangement also has an advantage in terms of sidelobe suppression in that, for all steering angles, the required excitation of the added elements is available from the oscillators immediately adjacent to those connected to the end radiating elements of the aperture. As indicated, this excitation must also be (antisymmetrically) shifted by an additional 90 degrees to align the interferometer zeros with those of the pattern of the original array. Beam-steering is controlled by the tuning voltages applied to the end oscillators of the array, V_T , while positioning of the sidelobe suppression region is controlled by the ganged attenuators, which determine the amplitude of the interferometer pattern of the end elements. The ganged switches on the 180-degree hybrids switch the suppression region from one side of the main lobe to the other.

III. A Two Dimensional Array with Uniform Illumination.

The two-dimensional arrays described by Kott comprise a number of one-dimensional arrays placed side by side. Here, in contradistinction, a two-dimensional array is described which provides a fully agile pencil beam and a fully steerable sidelobe suppression region, which can be positioned as desired in a far zone hemisphere.

A. Sidelobe Suppression.

In analogy with (1), the far zone field of the two-dimensional array may be written in the form,

$$E(\theta, \phi) = \sum_{m=-M}^M \sum_{n=-N}^N A_{mn} e^{-jms_x u(\theta, \phi)} e^{-jns_y v(\theta, \phi)} \quad (13)$$

where

$$u(\theta, \phi) = \sin \theta \cos \phi - \sin \theta_B \cos \phi_B$$

$$v(\theta, \phi) = \sin \theta \sin \phi - \sin \theta_B \sin \phi_B$$

and, for uniform illumination, $A_{mn}=1$. Again, summing in closed form one arrives at,

$$E(\theta, \phi) = \left\{ \frac{\sin[(M + \frac{1}{2})ks_x u(\theta, \phi)]}{\sin[\frac{1}{2}ks_x u(\theta, \phi)]} \right\} \left\{ \frac{\sin[(N + \frac{1}{2})ks_y v(\theta, \phi)]}{\sin[\frac{1}{2}ks_y v(\theta, \phi)]} \right\} \quad (14)$$

For sidelobe cancellation, four linear arrays are now added to the original two-dimensional array. These arrays are equal in length and number of elements to the edges of the original array and located half the inter-element spacing from the edge elements as shown by the circles in Figure 9 for $M=3$ and $N=2$. The excitation of these added elements is given by the following formulas.

For the array at $x = -(M + \frac{1}{2})s_x$, the excitations, f_n^- , are,

$$f_n^- = e^{-j(M + \frac{1}{2})ks_x \sin \theta_B \cos \phi_B} e^{j\left(\frac{\pi}{2}\right)} e^{jnks_y \sin \theta_B \sin \phi_B} \text{ for } -N \leq n \leq N \quad (15a)$$

For the array at $x = (M + \frac{1}{2})s_x$, the excitations, f_n^+ , are,

$$f_n^+ = e^{j(M + \frac{1}{2})ks_x \sin \theta_B \cos \phi_B} e^{-j\left(\frac{\pi}{2}\right)} e^{jnks_y \sin \theta_B \sin \phi_B} \text{ for } -N \leq n \leq N \quad (15b)$$

For the array at $y = -(N + \frac{1}{2})s_y$, the excitations, g_m^- , are,

$$g_m^- = e^{-j(N + \frac{1}{2})ks_y \sin \theta_B \sin \phi_B} e^{j\left(\frac{\pi}{2}\right)} e^{jmks_x \sin \theta_B \cos \phi_B} \text{ for } -M \leq m \leq M \quad (15c)$$

For the array at $y = (N + \frac{1}{2})s_y$, the excitations, g_m^+ , are,

$$g_m^+ = e^{j(N+\frac{1}{2})ks_y \sin \theta_B \sin \phi_B} e^{-j\left(\frac{\pi}{2}\right)} e^{jNks_x \sin \theta_B \cos \phi_B} \text{ for } -M \leq m \leq M \quad (15d)$$

With these excitations, the far zone fields of the peripheral arrays will be,

$$\begin{aligned} F(\theta, \phi) &= 2 \sin\left[\left(M + \frac{1}{2}\right)ks_x u(\theta, \phi)\right] \left\{ \frac{\sin\left[\left(N + \frac{1}{2}\right)ks_y v(\theta, \phi)\right]}{\sin\left[\frac{1}{2}ks_y v(\theta, \phi)\right]} \right\} \\ G(\theta, \phi) &= 2 \sin\left[\left(N + \frac{1}{2}\right)ks_y v(\theta, \phi)\right] \left\{ \frac{\sin\left[\left(M + \frac{1}{2}\right)ks_x u(\theta, \phi)\right]}{\sin\left[\frac{1}{2}ks_x u(\theta, \phi)\right]} \right\} \end{aligned} \quad (16)$$

Representing the total field, E_T , in the form,

$$E_T(\theta, \phi) = E(\theta, \phi) + P(\theta_s, \phi_s)F(\theta, \phi) + Q(\theta_s, \phi_s)G(\theta, \phi) \quad (17)$$

it becomes clear that sidelobe suppression centered at (θ_s, ϕ_s) will result if,

$$\begin{aligned} P(\theta_s, \phi_s) &= -\frac{\alpha}{2} \csc\left[\frac{1}{2}ks_x u(\theta_s, \phi_s)\right] \\ Q(\theta_s, \phi_s) &= -\frac{\beta}{2} \csc\left[\frac{1}{2}ks_y v(\theta_s, \phi_s)\right] \end{aligned} \quad (18)$$

where $\alpha + \beta = 1$ for which the total far zone field becomes,

$$\begin{aligned}
E(\theta, \phi) = & \left\{ \frac{\sin[(M + \frac{1}{2})ks_x u(\theta, \phi)]}{\sin[\frac{1}{2}ks_x u(\theta, \phi)]} \right\} \left\{ \frac{\sin[(N + \frac{1}{2})ks_y v(\theta, \phi)]}{\sin[\frac{1}{2}ks_y v(\theta, \phi)]} \right\} \\
& - \alpha \left\{ \frac{\sin[(M + \frac{1}{2})ks_x u(\theta, \phi)]}{\sin[\frac{1}{2}ks_x u(\theta_s, \phi_s)]} \right\} \left\{ \frac{\sin[(N + \frac{1}{2})ks_y v(\theta, \phi)]}{\sin[\frac{1}{2}ks_y v(\theta, \phi)]} \right\} \\
& - \beta \left\{ \frac{\sin[(M + \frac{1}{2})ks_x u(\theta, \phi)]}{\sin[\frac{1}{2}ks_x u(\theta, \phi)]} \right\} \left\{ \frac{\sin[(N + \frac{1}{2})ks_y v(\theta, \phi)]}{\sin[\frac{1}{2}ks_y v(\theta_s, \phi_s)]} \right\}
\end{aligned} \tag{19}$$

This pattern exhibits an agile beam pointed in the (θ_B, ϕ_B) direction and an independently steerable sidelobe suppression region including the direction (θ_s, ϕ_s) . From (19) it can be seen that this suppression region will lie along a curve defined by the following equation in the angular space.

$$\alpha \left\{ \frac{\sin[\frac{1}{2}ks_x u(\theta, \phi)]}{\sin[\frac{1}{2}ks_x u(\theta_s, \phi_s)]} \right\} + (1 - \alpha) \left\{ \frac{\sin[\frac{1}{2}ks_y v(\theta, \phi)]}{\sin[\frac{1}{2}ks_y v(\theta_s, \phi_s)]} \right\} = 1 \tag{20}$$

This curve obviously passes through $(\theta, \phi) = (\theta_s, \phi_s)$ regardless of the value of α . As α varies, the curve rotates around (θ_s, ϕ_s) as shown in Figure 10a for the case when $\theta_s = 30^\circ$ and $\phi_s = 30^\circ$. The arrow indicates the location of the point (θ_s, ϕ_s) . The curves passing through the point $(30^\circ, 210^\circ)$ are accessible by reversing the sign of the perimeter excitations relative to the original array. For large values of α (positive or negative) the limiting curves pass through both $(30^\circ, 30^\circ)$ and $(30^\circ, 210^\circ)$. From the definition of u and v one can easily see that scanning the main beam merely produces a shift in the u, v plane. Thus, it is clear that under scanning the two intersection points move in a manner similar to the motion of the beam. Therefore, by varying θ_s, ϕ_s , and α , one may position the suppression region to cover any two desired points in the hemisphere and, of course, the rest of the points along the corresponding curve defined by (20). The suppression described by Kott is recovered by setting α equal to 0 for a horizontal null or 1 for a vertical null.

Figure 10b shows the effect of moving the suppression region position (θ_s, ϕ_s) closer to the x -axis. Note that all of the contours except the two for $\alpha=1$ move toward horizontal. In fact, if (θ_s, ϕ_s) is placed on the x -axis, all of the contours except those for $\alpha=1$ become horizontal, coincide, and pass through the main beam. In general, this will occur whenever the line between (θ_B, ϕ_B) and (θ_s, ϕ_s) is horizontal and a similar phenomenon occurs when this line is vertical.

B. Numerical Examples.

Four examples are presented to illustrate the independent nature of the steering of the main beam and the suppression region in two dimensions. A 21×21 element array with

half wavelength element spacing is considered. Four 21 element linear arrays are added one-quarter wavelength from each edge. The first example far zone field, shown in Figure 11, illustrates the case in which the main beam is unscanned and the suppression region is set to pass through $(\theta_s, \phi_s) = (30^\circ, 30^\circ)$ and $\alpha = \frac{1}{2}$ placing the suppression region primarily in the first quadrant. The corresponding curve from Figure 10a is superimposed on the plot indicating that the suppression region follows the expected trajectory and the "X" locates (θ_s, ϕ_s) .

The second example, shown in Figure 12, illustrates a case in which the main beam is scanned to $(\theta_B, \phi_B) = (30^\circ, 180^\circ)$ while the suppression region is centered at $(\theta_s, \phi_s) = (30^\circ, 30^\circ)$ and $\alpha = \frac{5}{4}$. Here, again, the expected trajectory from (20) is superimposed and "X" locates (θ_s, ϕ_s) . Similarly, the third example, shown in Figure 13, illustrates a case in which the main beam is scanned to $(\theta_B, \phi_B) = (30^\circ, 180^\circ)$ while the suppression region is centered at $(\theta_s, \phi_s) = (30^\circ, 0^\circ)$. For this case α must be unity because Q in (18) becomes infinite. This is a case of the sort discussed previously by Kott. The fact that there are two nearby nulling contours rather than just one is due to very small numerical inaccuracies. Finally, Figure 14 illustrates a more general case in which the main beam is scanned to $(\theta_B, \phi_B) = (30^\circ, 60^\circ)$ while the suppression region is centered at $(\theta_s, \phi_s) = (30^\circ, -45^\circ)$ and $\alpha = \frac{1}{4}$. These examples indicate the overall performance achieved with this two dimensional generalization of the Kott scheme.

IV. Concluding Summary.

It has been shown that, under the assumption of uniform aperture illumination, the sidelobe suppression concept due to Kott can be conveniently and optimally implemented in an array using the coupled oscillator aperture phase control scheme of Liao and York. Moreover, the two-dimensional generalization of the coupled oscillator scheme analyzed by Pogorzelski has been shown to provide for a two-dimensional generalization of the Kott scheme resulting in a two-dimensional array with independently steerable main beam and sidelobe suppression region.

Acknowledgments.

Thanks are due Dr. Robert Mailloux of the Air Force Research Laboratories for calling my attention to the work of Tseng. The research described in this paper was performed by the Center for Space Microelectronics Technology, Jet Propulsion Laboratory, California Institute of Technology, and was partially sponsored by the Ballistic Missile Defense Organization through an agreement with the National Aeronautics and Space Administration.

References:

1. M. A. Kott, U.S. Patent 5,343,211, "Phased Array with Wide Null," August 30, 1994.
2. F. I. Tseng, "Design of Array and Line-Source Antennas for Taylor Patterns with a Null," IEEE Trans. Antennas Propagat., AP-27, 474-479, July 1979.
3. P. Liao and R. A. York, "A New Phase-Shifterless Beam-Scanning Technique Using Arrays of Coupled Oscillators," IEEE Trans. Microwave Theory and Tech., MTT-41, 1810-1815, October 1993.
4. R. J. Pogorzelski, P. F. Maccarini, and R. A. York, "A Continuum Model of the Dynamics of Coupled Oscillator Arrays for Phase-Shifterless Beam Scanning," IEEE Trans. Microwave Theory and Tech., MTT-47, 463-470, April 1999.
5. R. J. Pogorzelski, "On the Dynamics of Two-Dimensional Array Beam Steering via Perimeter Detuning of Coupled Oscillator Arrays," submitted to IEEE Trans. Antennas Propagat., Jan. 1999.

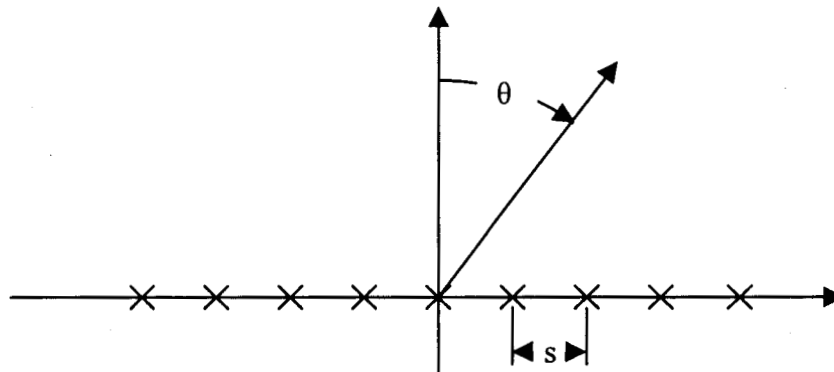


Figure 1. Linear array of isotropic elements.

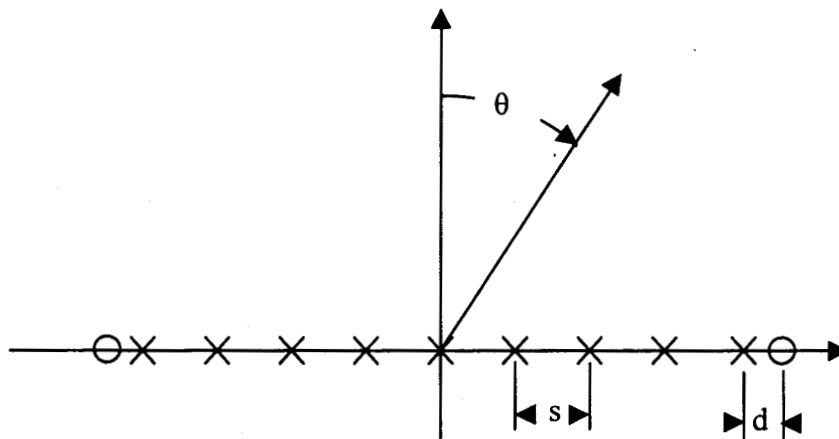


Figure 2. Augmented array of isotropic elements.

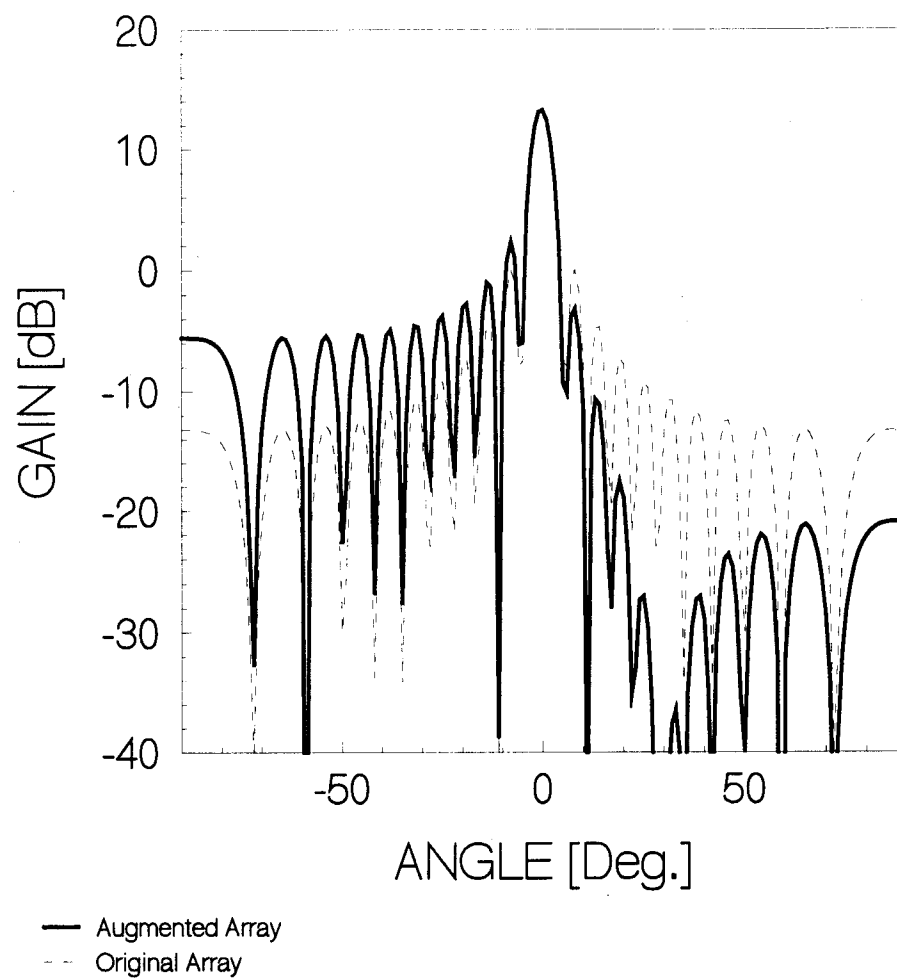


Figure 3a. Sidelobe suppression at 30 degrees for an unscanned beam.

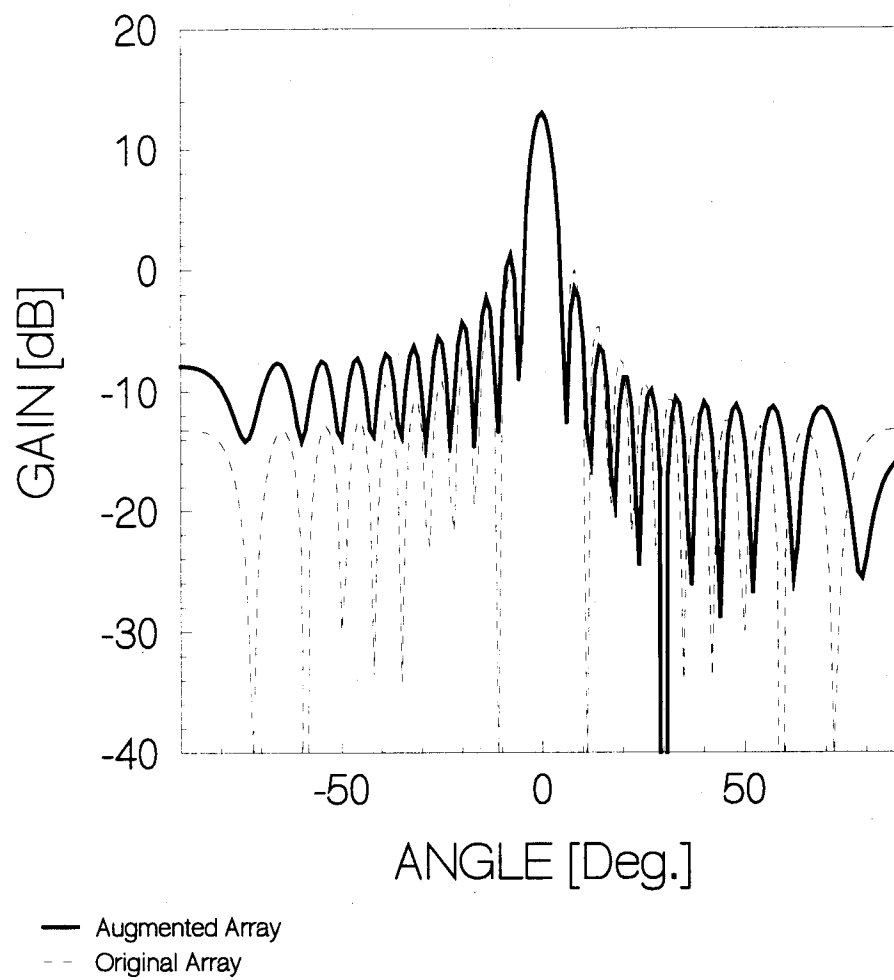


Figure 3b. Sidelobe cancellation at 30 degrees via one added element.

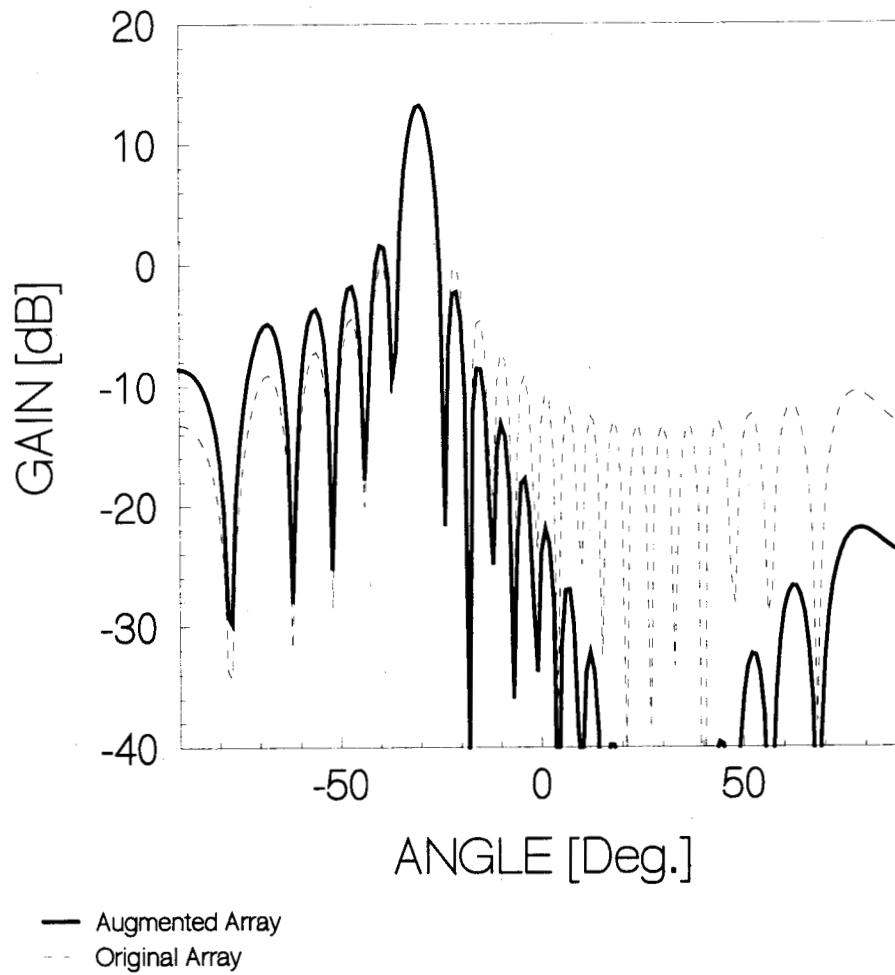


Figure 4. Sidelobe suppression at 30 degrees with main beam scanned to -30 degrees.

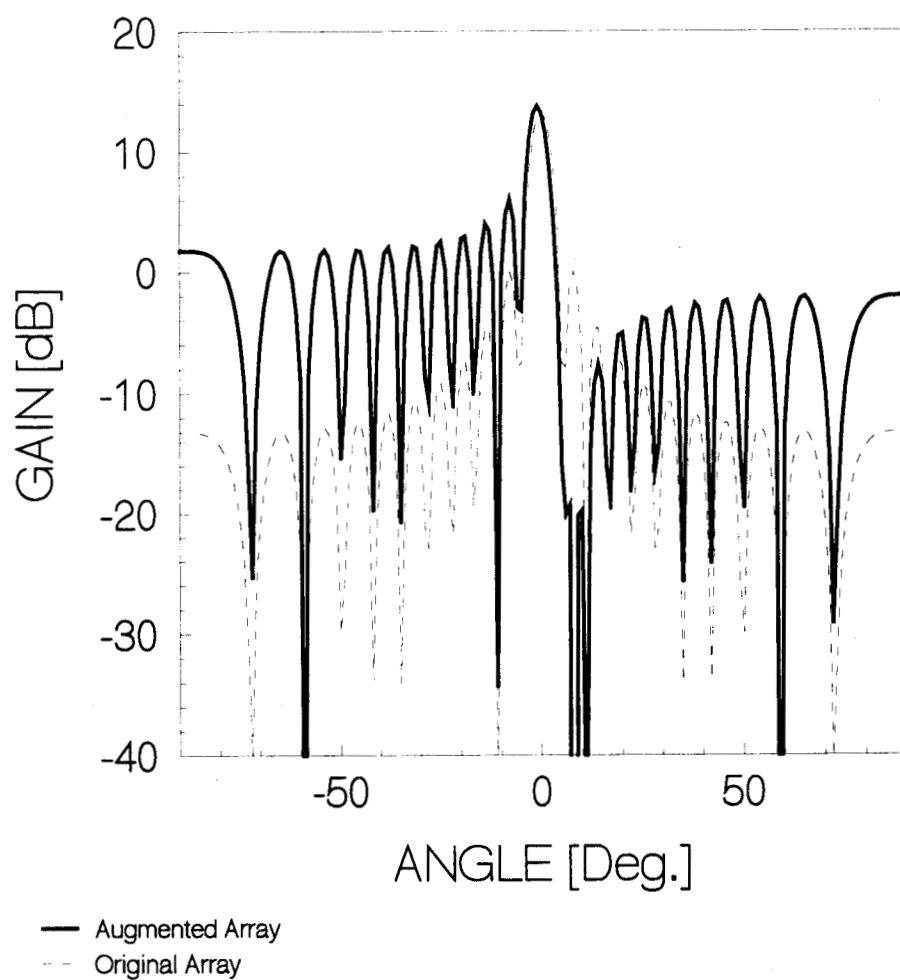


Figure 5. Sidelobe suppression at 8 degrees for an unscanned beam.

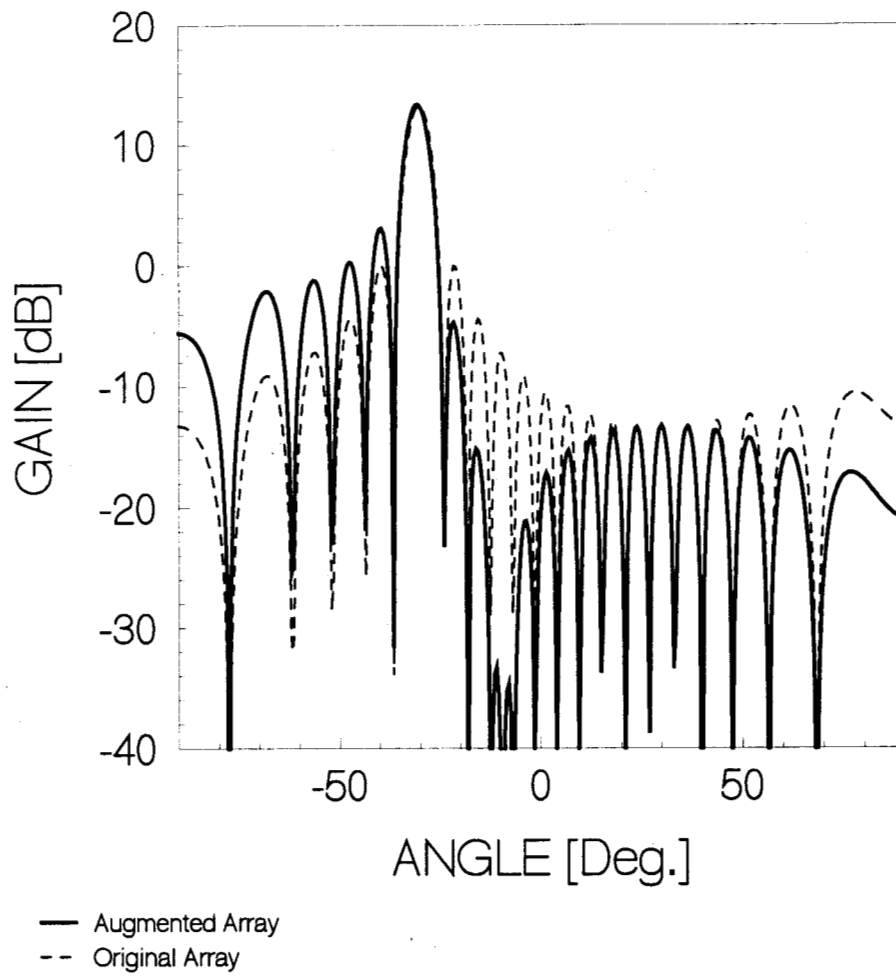


Figure 6. Sidelobe suppression for no increase in sidelobe level to the right of the main beam at -30 degrees.

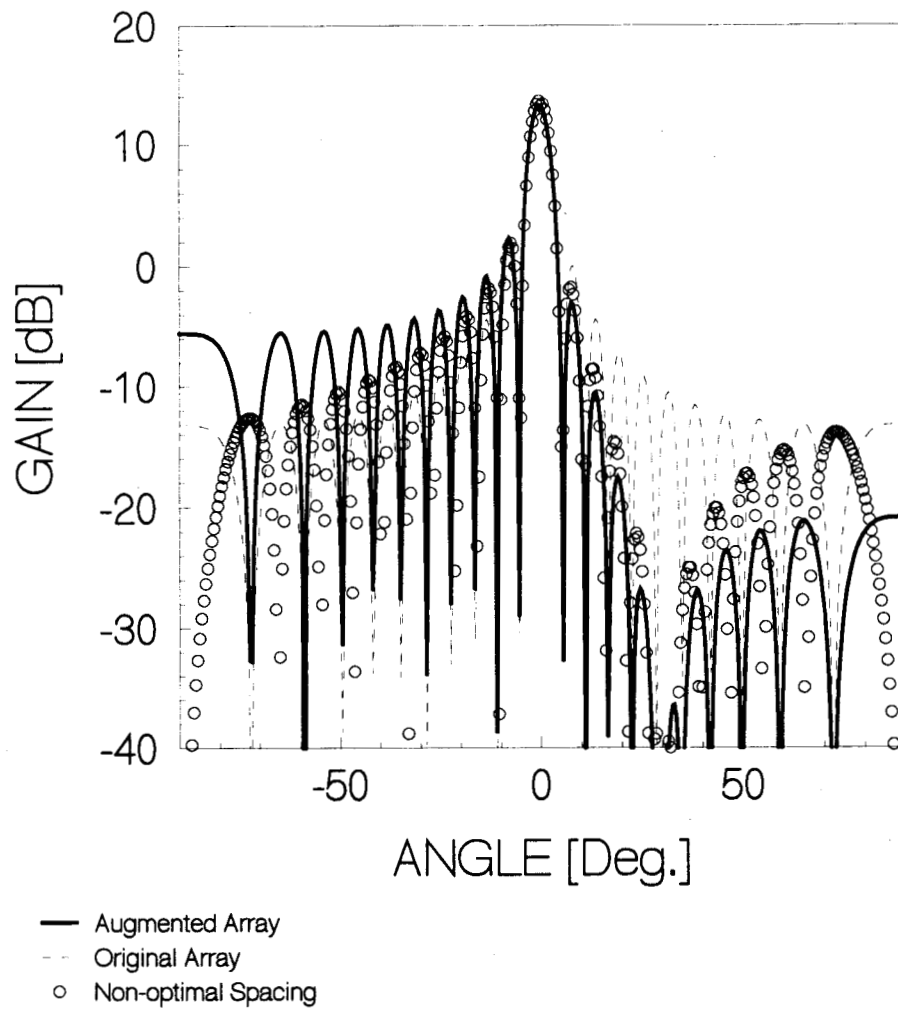


Figure 7. Comparison of optimal and non-optimal element spacing for the case of Figure 3.

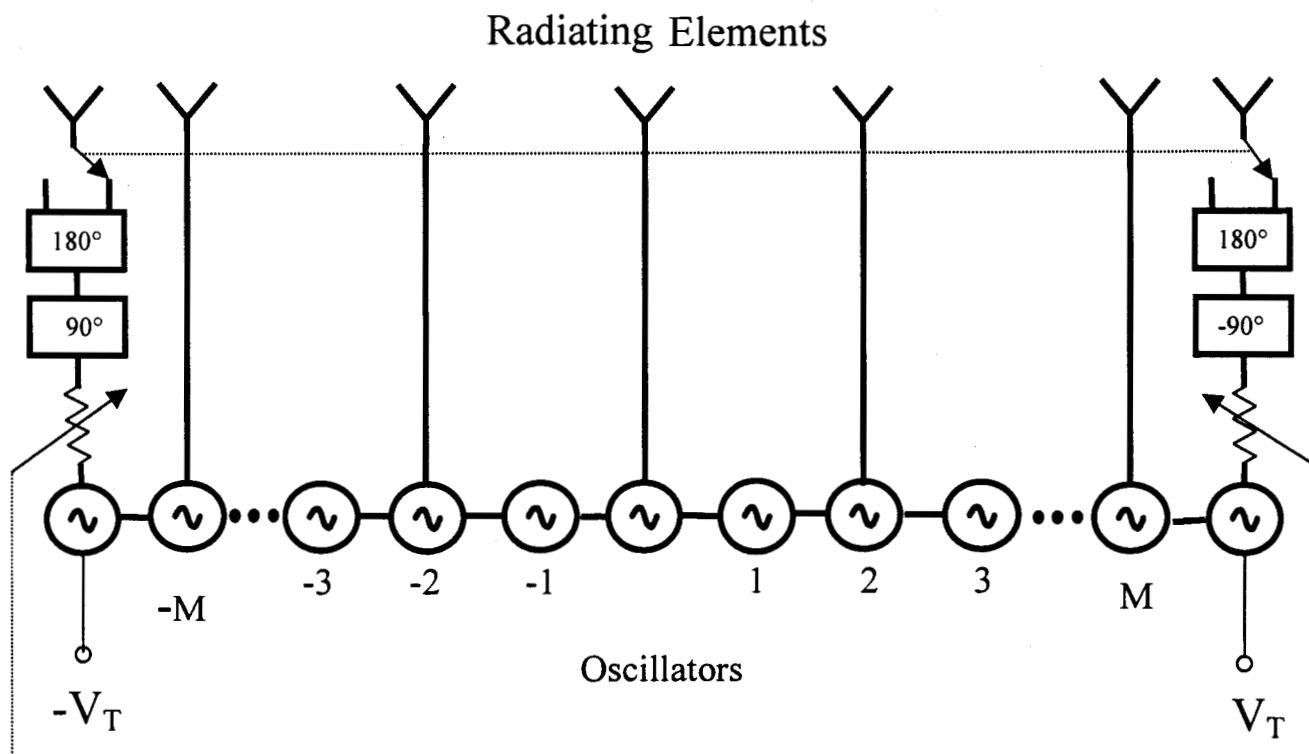


Figure 8. Coupled oscillator controlled array with sidelobe suppression.

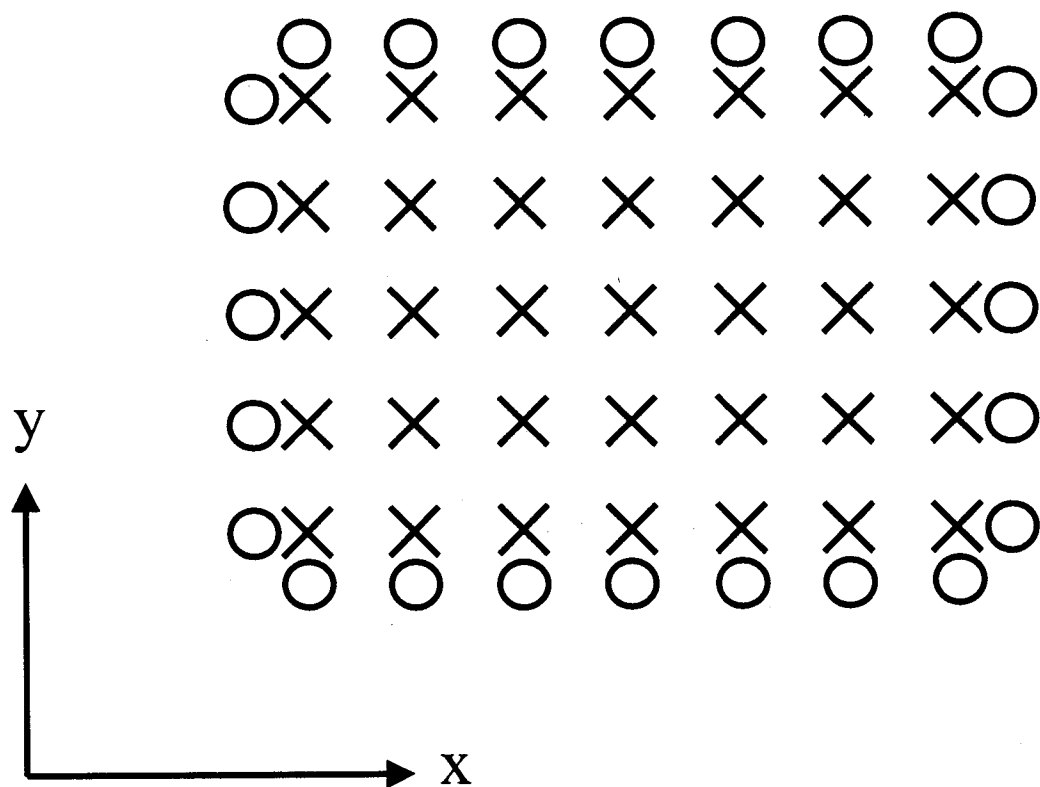


Figure 9. Two-dimensional array with linear sidelobe canceling arrays.

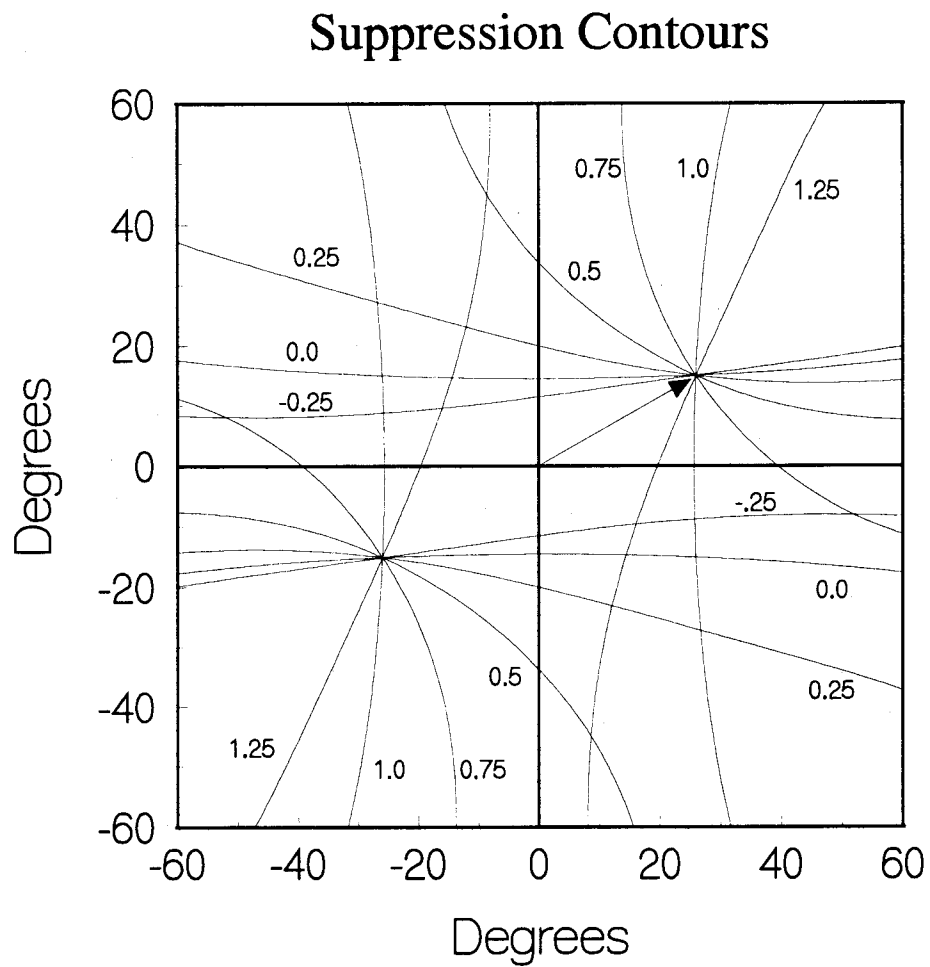


Figure 10a. Trajectories of the suppression region for various values of α when the suppression region is centered at $(30^\circ, 30^\circ)$ and the beam is unscanned.

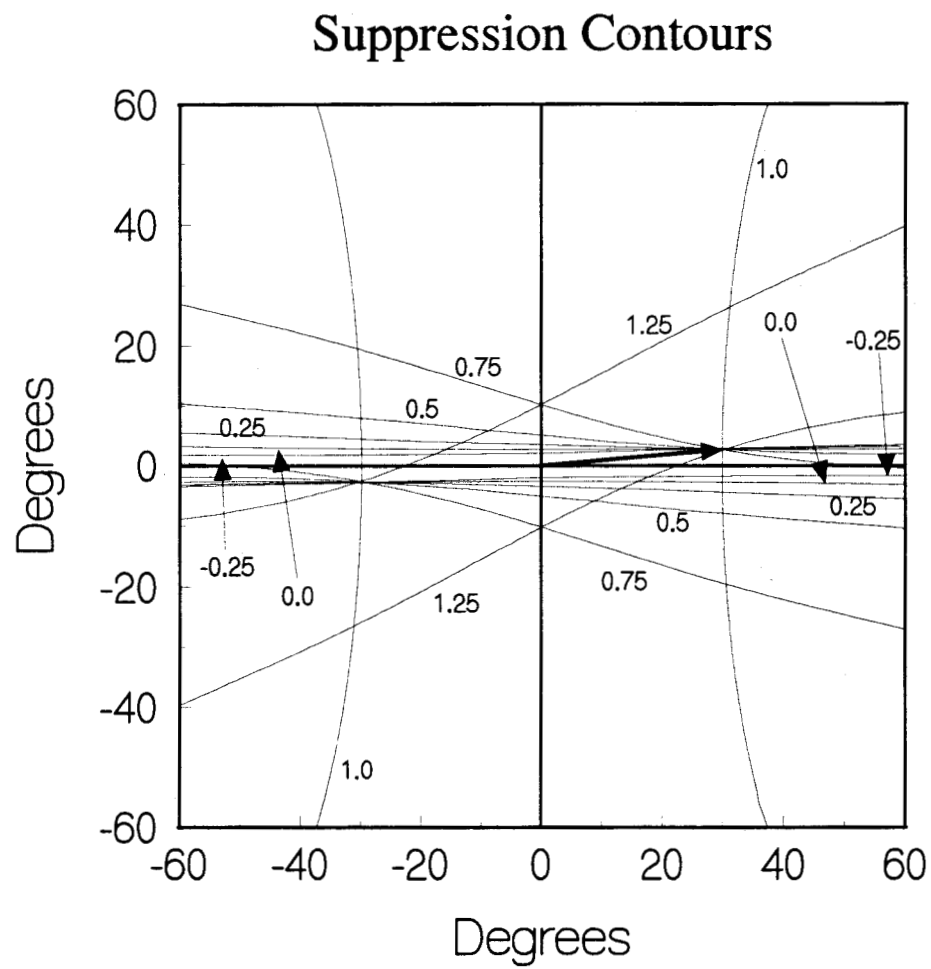


Figure 10b. Trajectories of the suppression region for various values of α when the suppression region is centered at $(30^\circ, 5^\circ)$ and the beam is unscanned.

SIDELOBE CANCELLATION

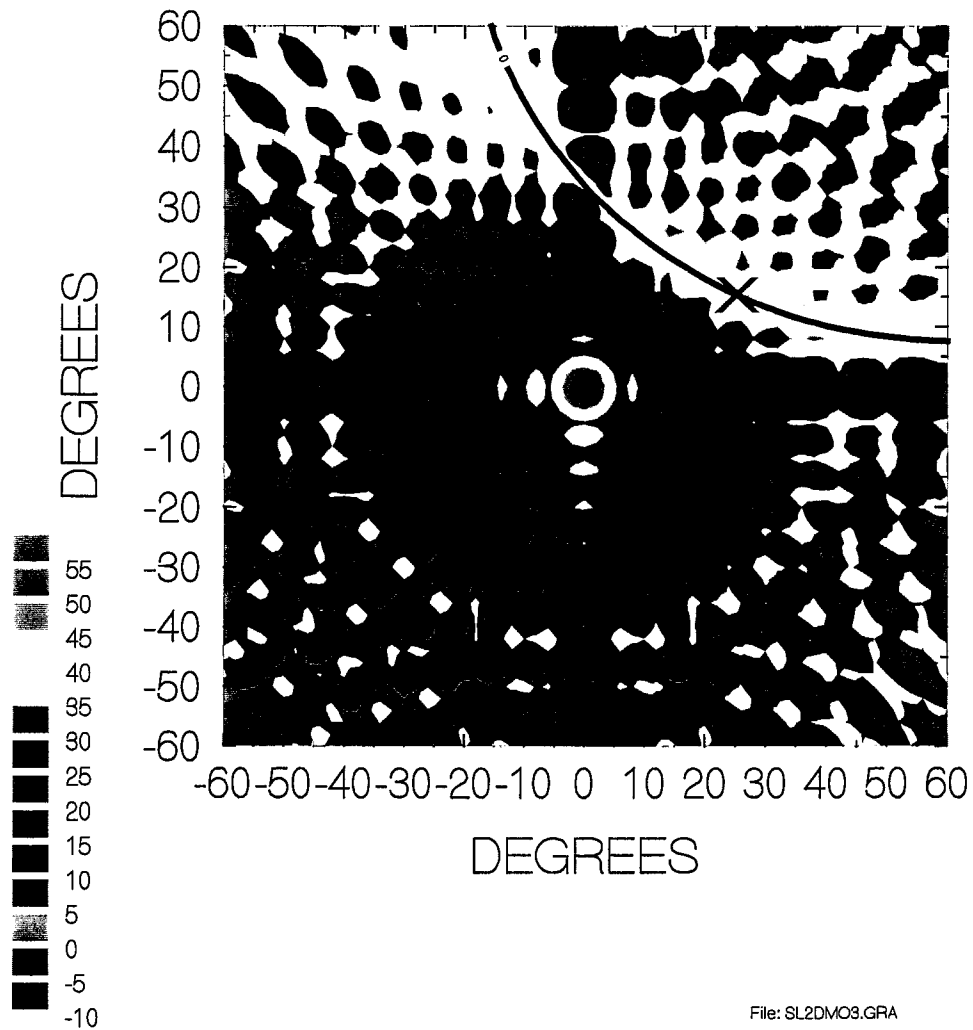


Figure 11. Far zone pattern of a two dimensional array with uns scanned main beam having sidelobes suppressed in the first quadrant.

SIDELOBE CANCELLATION

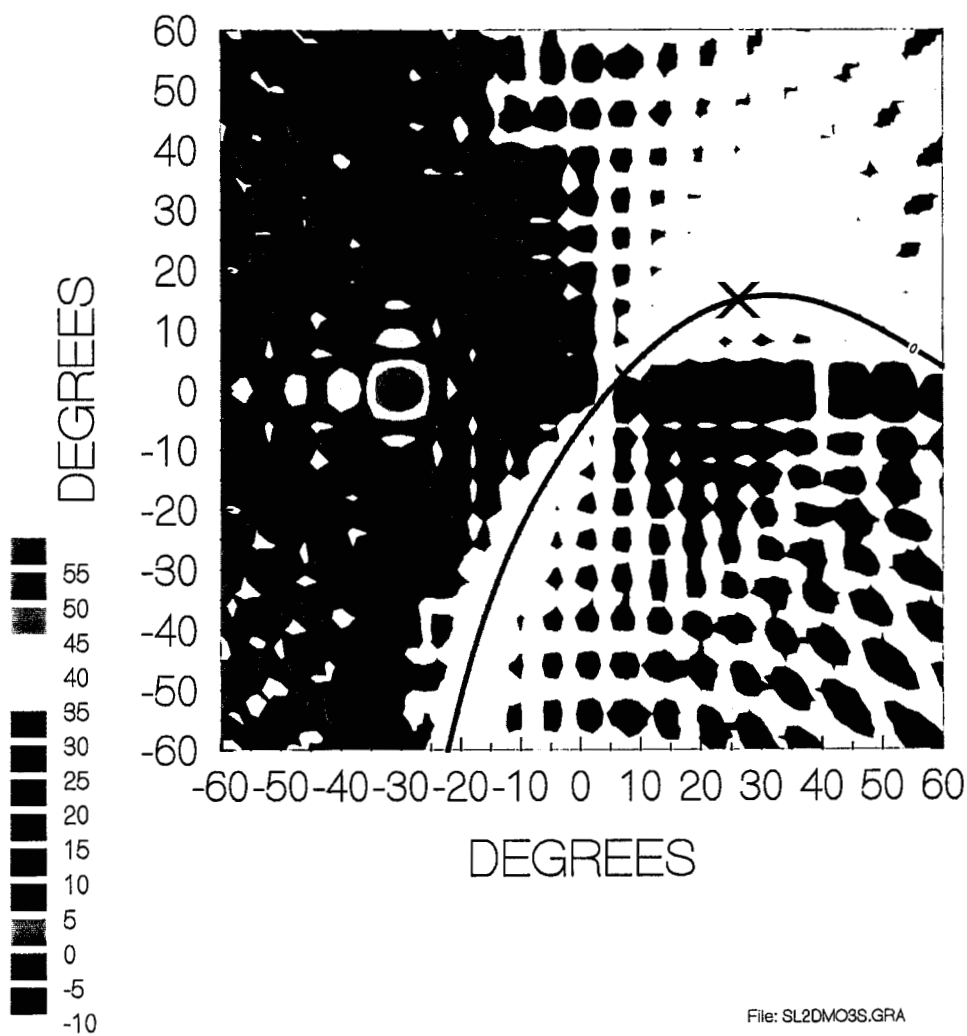


Figure 12. Far zone pattern of a two dimensional array with scanned main beam having sidelobes suppressed in the first quadrant and $\alpha = \frac{\pi}{4}$.

SIDELOBE CANCELLATION

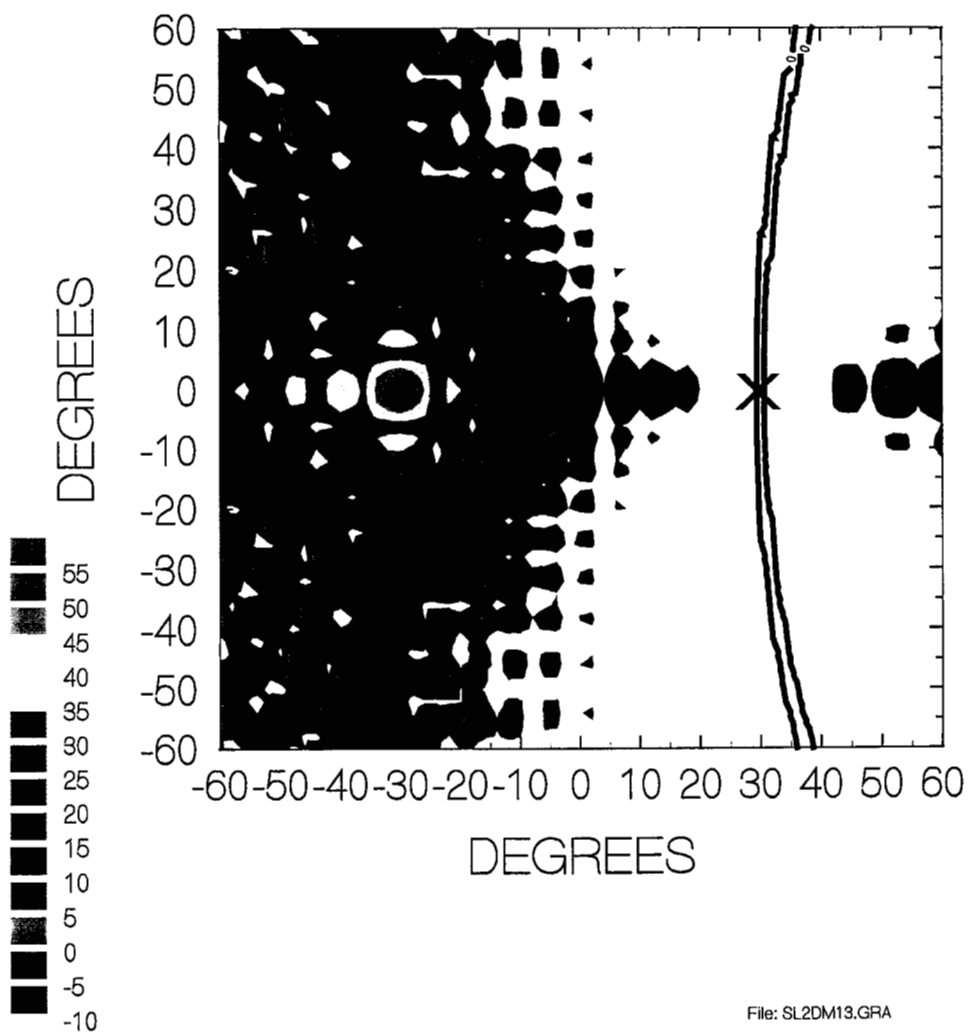


Figure 13. Far zone pattern of a two dimensional array with scanned main beam having sidelobes suppressed in the first quadrant.

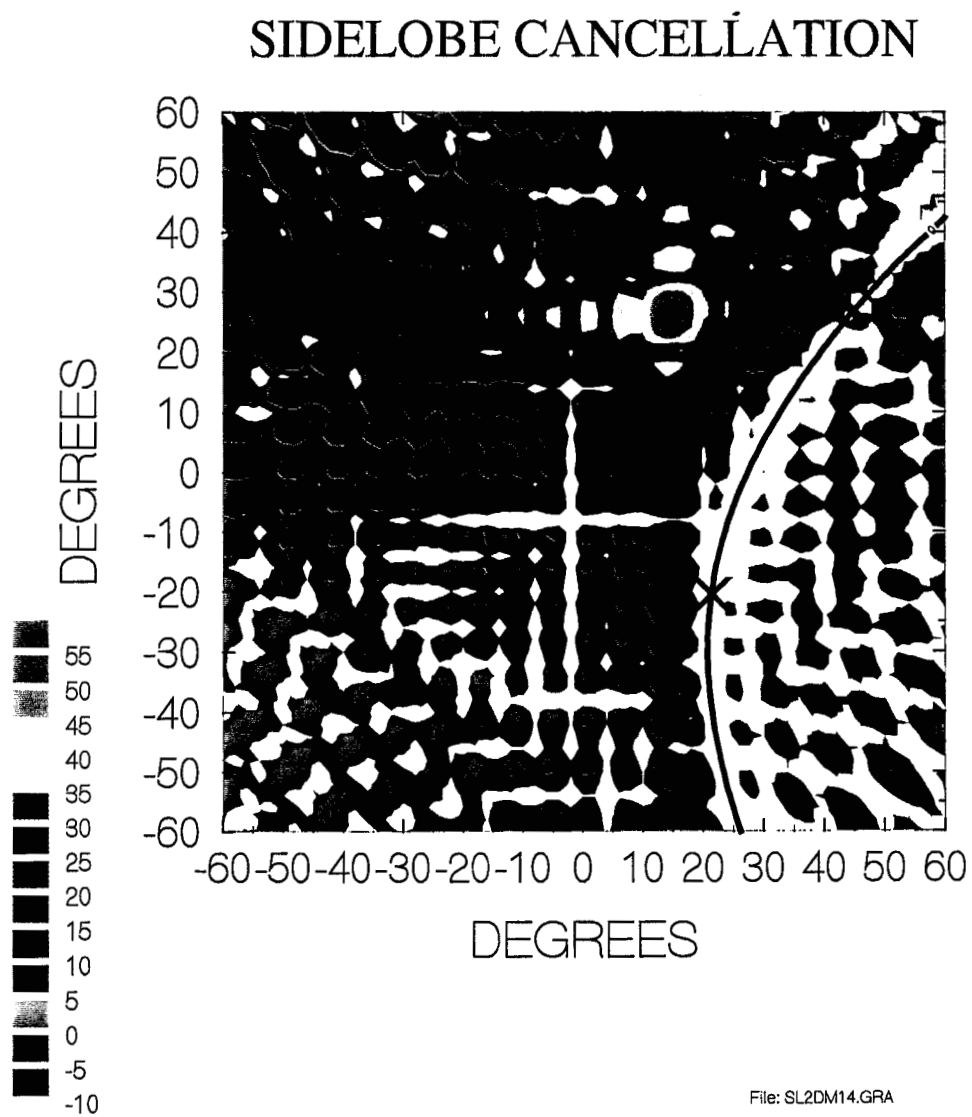


Figure 14. Far zone pattern of a two dimensional array with scanned main beam having sidelobes suppressed in the fourth quadrant.



On a Simple Method of Obtaining Sidelobe Reduction over a Wide Angular Range in One and Two Dimensions

Ronald J. Pogorzelski
Jet Propulsion Laboratory
California Institute of Technology

The research described in this paper was performed by the Center for Space Microelectronics Technology, Jet Propulsion Laboratory, California Institute of Technology, and was partially supported by the Ballistic Missile Defense Organization through an agreement with the National Aeronautics and Space Administration.

A patented technique for suppressing the sidelobes of an array antenna is considered. This technique involves the addition of two elements, one at each end of the array, which together produce an interferometer pattern used for cancellation of sidelobes. It is shown here that the technique is most effective for uniform illumination and that there then exists an optimum fixed position for the added elements. The amplitude of the excitation of the auxiliary elements determines the angular location of the region of sidelobe reduction while the phase of the excitation tracks the beam-steering phase of the array. Thus, this technique is seen to be easily implemented in an array controlled by coupled oscillators. The technique generalizes in a straightforward manner to two-dimensional arrays in which case a set of auxiliary elements on the perimeter of the array is required. A two dimensional oscillator controlled array of this type is described here with which one can produce a main beam and a sidelobe suppression region which can be independently positioned anywhere in a hemisphere provided they do not coincide.



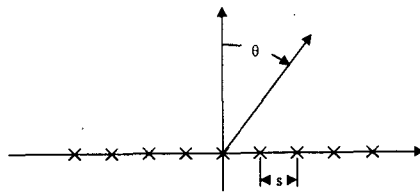
Agenda

- Michael Kott's Patent.
- Optimal element positioning in one dimension.
 - Uniform and non-uniform tapers.
 - Tseng's work.
 - Coupled oscillator implementation.
- Generalization to two dimensions.
 - Suppression contours.
 - Coupled oscillator implementation.
- Concluding Summary.

The presentation will begin with a discussion of Kott's patent on a method of sidelobe suppression. It will be shown that it works best with uniform illumination taper and that in such a case there is an optimum location for the radiating elements added to the array. This result will be shown to be consistent with the results of Tseng which indicate that sidelobe suppression in a one-dimensional array can be achieved by modification of the excitation of the only the elements at or near the ends of the array. Implementation of Kott's scheme using coupled oscillator array phase control is then discussed and it is found that such an implementation is very well suited to the Kott scheme.

The Kott approach will then be generalized to two-dimensional arrays. Two-dimensional arrays are actually considered in the patent but only in a limited fashion. The full generality available is discussed here. Again, coupled oscillator phase control is shown to be a convenient method of implementation.

JPL Linear Array of Isotropic Elements



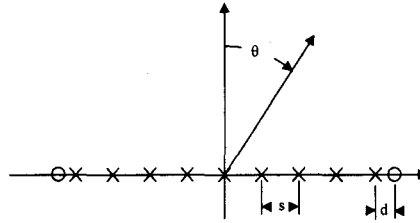
$$E(\theta) = \frac{\sin[(M + \frac{1}{2})ksu(\theta)]}{\sin[\frac{1}{2}ksu(\theta)]}$$

$$u(\theta) = \sin \theta - \sin \theta_B$$

We begin by considering the linear array of isotropic elements shown here. The radiation pattern exhibits the familiar $\sin(x)/x$ behavior of a uniform aperture distribution.

JPL

Augmented Array



$$E_T(\theta) = \frac{\sin\left[\left(M + \frac{1}{2}\right)ksu(\theta)\right]}{\sin\left[\frac{1}{2}ksu(\theta)\right]} + P_- e^{jp_-} e^{jk(Ms+d)\sin\theta} + P_+ e^{jp_+} e^{-jk(Ms+d)\sin\theta}$$

Following Kott, we augment the array by adding two more elements, one at each end and seek an optimum excitation of these elements to produce suppression of the pattern in the vicinity of a specified angle in the sidelobe region.



Sidelobe Cancellation

GOAL:

Set d , P 's, and p 's to cancel sidelobes in a specified region. Choose,

$$d = \frac{s}{2}$$

$$p = -\frac{\pi}{2} + (M + \frac{1}{2})ks \sin \theta_B$$

$$P = \frac{1}{2 \sin[\frac{1}{2} ks(\sin \theta_s - \sin \theta_B)]} = \frac{1}{2 \sin[\frac{1}{2} ksu(\theta_s)]}$$

The two added elements form an interferometer exhibiting the usual uniform amplitude pattern of lobes. By properly choosing the distance d and the amplitude and phase of the excitations, one may match the interferometer lobe width to that of the array pattern in the sidelobe region. Then, by adjustment of the amplitude of the excitation of the added elements, one may cancel the array pattern over a relatively wide angular region surrounding any desired point.



Cancellation (Continued)

Then,

$$E_T(\theta) = \frac{\sin[(M + \frac{1}{2})ksu(\theta)]}{\sin[\frac{1}{2}ksu(\theta)]} - \frac{\sin[(M + \frac{1}{2})ksu(\theta_s)]}{\sin[\frac{1}{2}ksu(\theta_s)]}$$

or,

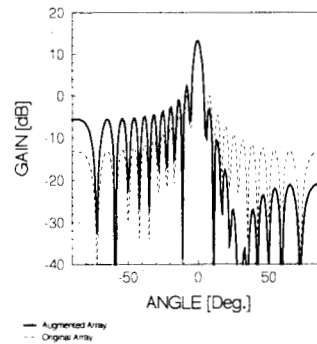
$$E_T(\theta) = \{ \csc[\frac{1}{2}ksu(\theta)] - \csc[\frac{1}{2}ksu(\theta_s)] \} \{ \sin[(M + \frac{1}{2})ksu(\theta)] \}$$

The far zone pattern of the augmented array may then be expressed as shown here.

To illustrate the effectiveness of the technique described above, we compute a number of simple examples and plot the far zone gain of the array. The array to be considered is a 21-element array ($M=10$) with half wavelength spacing. The two added elements are then spaced one-quarter wavelength from the end elements.

Example 1

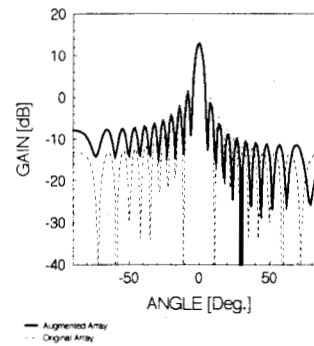
- 21 element array
- $\lambda/2$ spacing
- Unscanned beam
- S/L cancelled at 30°
- Optimum added element spacing



We begin with the case of an unscanned beam and select the suppression region to be centered at 30 degrees from broadside. The resulting pattern is shown here together with the pattern of the original array without the added elements. Note that the suppression extends over several sidelobes. Note also that, because the pattern of the added elements is antisymmetric, the sidelobes for negative angles are enhanced.

Example 1a

- 21 element array
- $\lambda/2$ spacing
- Unscanned beam
- S/L cancelled at 30°
- Single added element

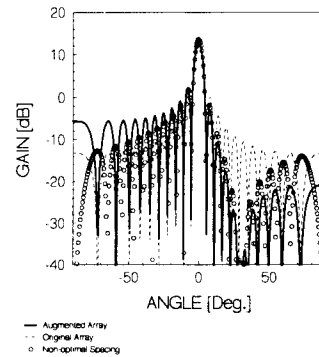


The preceding result is to be compared with the traditional nulling technique using a single added element weighted to place a null at 30 degrees. The result is shown here and exhibits a much narrower suppression region.

Kott's sidelobe suppression scheme has been applied here to a linear array with uniform illumination. It has been shown that if the separation of the added elements from the end elements of the array is set to exactly half the inter-element separation of the original array and if the phases of the added elements are set to a value which is linearly extrapolated from the phases of the original array elements and augmented appropriately by ± 90 degrees, the zeros of the pattern of the added elements exactly coincide with the zeros of the original array pattern. This will only be true for uniform illumination. It is in this sense that the uniform case is the ideal one for the Kott suppression scheme; that is, it yields the widest possible suppression region. For any other taper, the interferometer pattern must be adjusted to match the zeros where suppression is desired and will not match the zeros elsewhere in the pattern of the original array.

Example 1b

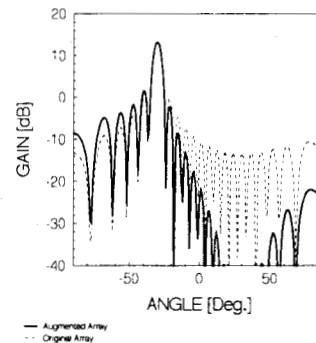
- 21 element array
- $\lambda/2$ spacing
- Unscanned beam
- S/L cancelled at 30°
- Non-optimal added element spacing: $d=s$



For example, Kott suggested that the added elements might be placed one inter-element spacing away from the end elements of the original array. If this is done and the phase, p , is adjusted to produce cancellation of the pattern at the desired suppression angle a somewhat degraded suppression centered at θ_s is obtained. As a specific example, consider the case in which the beam is unscanned and the suppression is centered at 30 degrees. This chart shows the result of using $d=s$ superimposed on the previously discussed patterns. Note that the width of the suppression region is reduced. However, the impact on the rest of the pattern is also reduced resulting in a lesser increase in sidelobe level than that resulting from the optimum element spacing. Of course, for any but uniform aperture illumination, one is left no choice but to adjust p for best alignment of the lobes for cancellation as described and spacing of the added elements is of lesser importance.

Example 2

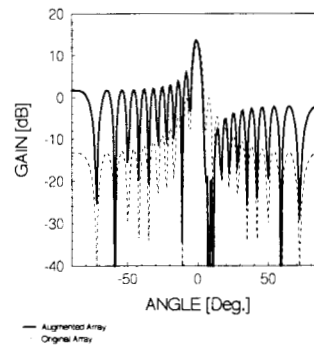
- 21 element array
- $\lambda/2$ spacing
- Beam scanned to -30°
- S/L cancelled at 30°
- Optimum added element spacing



Next, consider an array with the main beam steered to -30 degrees from broadside and apply sidelobe suppression centered at 30 degrees as before. Here the suppression is even more effective due to the greater angle between the main lobe and the suppression region. This implies that if the suppression region were chosen close to the main lobe, the suppression would be reduced in effectiveness.

Example 3

- 21 element array
- $\lambda/2$ spacing
- Unscanned beam
- S/L cancelled at 8°
- Optimum added element spacing
- Note increased neighboring sidelobes



This is verified in the case plotted here where the main lobe is unscanned but the suppression region is centered at 8 degrees. Here sidelobes for both positive and negative angles are enhanced and the suppression region is much narrower. Thus, the suppression is less effective near the main lobe and more effective far from the main lobe.

JPL Condition for No Increase in Neighboring Sidelobes

$$\csc\left[\frac{1}{2}ksu(\theta_s)\right]=2$$

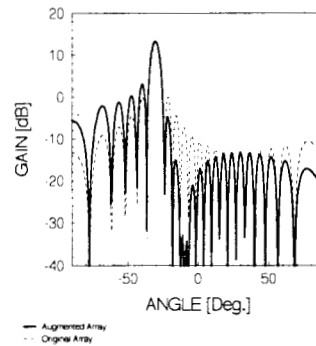
Which for the present
examples implies that:

$$\sin \theta_s - \sin \theta_B = \frac{1}{3}$$

The transition between these two extremes can be taken to occur when no sidelobes on the same side of the main beam as the suppression region are increased in level. The mathematical condition for this to occur is given here.

JPL No Neighboring Sidelobe Increase

- 21 element array
- $\lambda/2$ spacing
- Beam scanned to 30°
- S/L cancelled at 9.594°
- Optimum added element spacing



This transition case is illustrated here where the main beam is scanned to -30 degrees while, according to (11), the suppression region is centered at -9.594 degrees. As anticipated, none of the sidelobes to the right of the main beam are increased.

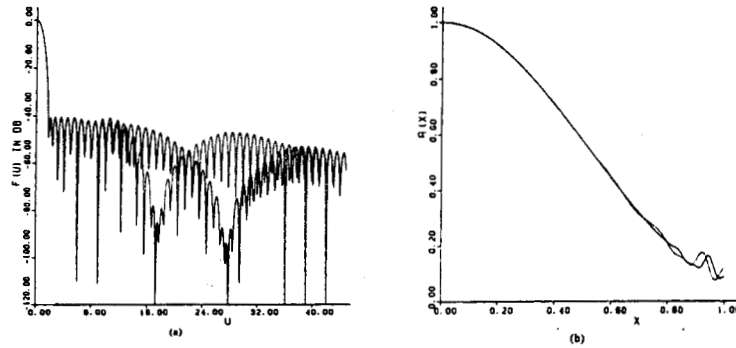
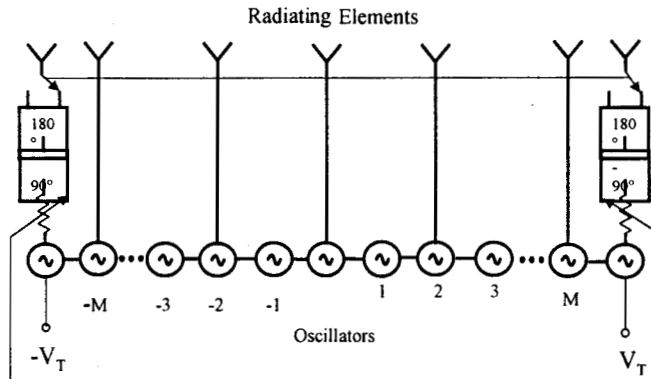


Fig. 5. (a) Null steering for $m_2 = 17$ (dashed) and $m_2 = 27$ (solid) with $R = 40$ dB, $B = 0.5$. (b) Aperture distribution for $m_2 = 17$ (dashed) and $m_2 = 27$ (solid) with $R = 40$ dB and $B = 0.5$.

Recalling Tseng's work [IEEE Trans. AP-27, 474-479, July 1979], one might at this point wonder why the necessary modification of the aperture distribution to achieve sidelobe suppression was found to lie not at the ends of the array but, rather, somewhat inside the aperture. After all, in the analysis above, placing the added elements at half the inter-element spacing from the end elements of the original array can be viewed as placing them at the outer edge of the last unit cell of the original array; i.e., at the aperture edge. The explanation is, of course, that Tseng's sidelobe suppression is symmetrical. That is, he creates a notch in the sidelobes on both sides of the beam whereas Kott's notch exists on only one side. Thus, the interferometer lobes of the added elements, which would normally have a null at the angle of the main beam, must be adjusted so as to slip one half cycle with respect to the sidelobes of the original array as one passes from one suppression region to the one on the opposite side of the main beam. This is accomplished by reducing the spacing of the added elements thus widening their interferometer lobes a bit. In fact, this places the added elements within the aperture of the original array. Further evidence of this can be found in Tseng's Figure 5. wherein it is shown that suppression closer to the main beam requires more extreme narrowing of the interferometer aperture; i.e. more extreme widening of the lobes, to achieve the phase reversal in the corresponding shorter angular range between suppression regions.

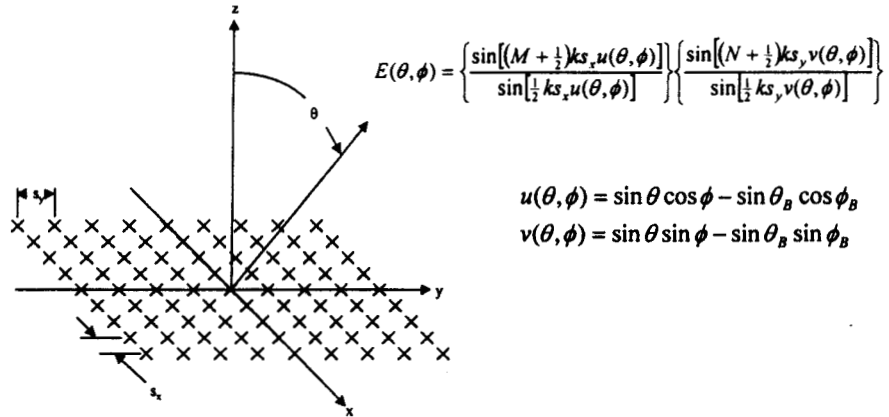
Coupled Oscillator Implementation



Recently, Liao and York introduced a method of beam-steering applicable to linear arrays using an array of coupled electronic oscillators to produce the necessary element excitations.[3] They showed that the beam of such an array could be electronically steered without the use of phase shifters by controlling the free running frequencies of the end oscillators of the oscillator array. Inherent in this concept, however, is the assumption of uniform oscillator amplitude throughout the array. As has been shown here, the uniform taper is, in a mathematical sense, the ideal taper for Kott's scheme and, in fact, the coupled oscillator system provides a means of achieving optimum results under the uniform aperture illumination assumption.

The system shown possesses several desirable features. The oscillators are assumed to be voltage controlled. That is, voltages applied to their tuning ports determine their free running frequencies. First, note that the phase difference between oscillators is limited to 90 degrees in order that the oscillators remain mutually injection locked as described by Liao and York. Thus, for half wavelength spacing of the radiating elements, if every oscillator is connected to a radiating element, the achievable beam-steering range is limited to plus and minus 30 degrees from boresight. However, if only every other oscillator is connected to a radiating element, this range extends to endfire. This arrangement also has an advantage in terms of sidelobe suppression in that, for all steering angles, the required excitation of the added elements is available from the oscillators immediately adjacent to those connected to the end radiating elements of the aperture. As indicated, this excitation must also be (antisymmetrically) shifted by an additional 90 degrees to align the interferometer zeros with those of the pattern of the original array. Beam-steering is controlled by the tuning voltages applied to the end oscillators of the array, V_T , while positioning of the sidelobe suppression region is controlled by the ganged attenuators, which determine the amplitude of the interferometer pattern of the end elements. The ganged switches on the 180-degree hybrids switch the suppression region from one side of the main lobe to the other.

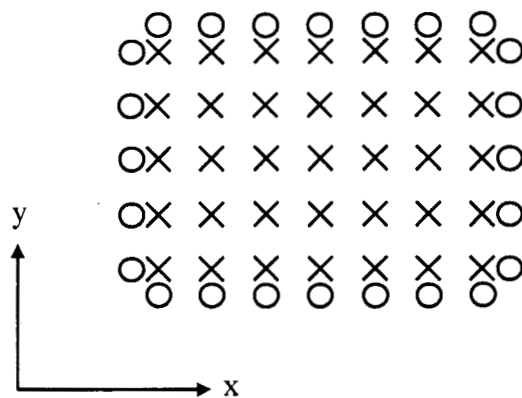
Two-Dimensional Array



16

The two-dimensional arrays described by Kott comprise a number of one-dimensional arrays placed side by side. Here, in contradistinction, a two-dimensional array is described which provides a fully agile pencil beam and a fully steerable sidelobe suppression region which can be positioned as desired in a far zone hemisphere.

Augmented Array



For sidelobe cancellation, four linear arrays are now added to the original two-dimensional array. These arrays are equal in length and number of elements to the edges of the original array and located half the inter-element spacing from the edge elements as shown by the circles for $M=3$ and $N=2$



Augmentation Excitations

$$f_n^- = e^{-j(M+\frac{1}{2})ks_x \sin \theta_B \cos \phi_B} e^{j\left(\frac{\pi}{2}\right)} e^{jnks_y \sin \theta_B \sin \phi_B} \text{ for } -N \leq n \leq N$$

$$f_n^+ = e^{j(M+\frac{1}{2})ks_x \sin \theta_B \cos \phi_B} e^{-j\left(\frac{\pi}{2}\right)} e^{jnks_y \sin \theta_B \sin \phi_B} \text{ for } -N \leq n \leq N$$

$$g_m^- = e^{-j(N+\frac{1}{2})ks_y \sin \theta_B \sin \phi_B} e^{j\left(\frac{\pi}{2}\right)} e^{jnks_x \sin \theta_B \cos \phi_B} \text{ for } -M \leq m \leq M$$

$$g_m^+ = e^{j(N+\frac{1}{2})ks_y \sin \theta_B \sin \phi_B} e^{-j\left(\frac{\pi}{2}\right)} e^{jnks_x \sin \theta_B \cos \phi_B} \text{ for } -M \leq m \leq M$$

The excitations of the added linear array elements are expressed in this form.



Augmentation Patterns

$$F(\theta, \phi) = 2 \sin\left[\left(M + \frac{1}{2}\right)ks_x u(\theta, \phi)\right] \left\{ \frac{\sin\left[\left(N + \frac{1}{2}\right)ks_y v(\theta, \phi)\right]}{\sin\left[\frac{1}{2}ks_y v(\theta, \phi)\right]} \right\}$$

$$G(\theta, \phi) = 2 \sin\left[\left(N + \frac{1}{2}\right)ks_y v(\theta, \phi)\right] \left\{ \frac{\sin\left[\left(M + \frac{1}{2}\right)ks_x u(\theta, \phi)\right]}{\sin\left[\frac{1}{2}ks_x u(\theta, \phi)\right]} \right\}$$

$$E_T(\theta, \phi) = E(\theta, \phi) + P(\theta_s, \phi_s)F(\theta, \phi) + Q(\theta_s, \phi_s)G(\theta, \phi)$$

The resulting radiation patterns of the two pairs of linear arrays are as shown and the total field of the augmented array is expressed as a linear combination of the fields of the original array and the those of the added linear arrays.



Sidelobe Suppression Weights

$$P(\theta_s, \phi_s) = -\frac{\alpha}{2} \csc\left[\frac{1}{2} k s_x u(\theta_s, \phi_s)\right]$$

$$Q(\theta_s, \phi_s) = -\frac{\beta}{2} \csc\left[\frac{1}{2} k s_y v(\theta_s, \phi_s)\right]$$

$$\alpha + \beta = 1$$

For sidelobe suppression in the two-dimensional case we set the P and Q to the value shown here under the condition at the bottom of the chart.



Total Field Pattern

$$E(\theta, \phi) = \left\{ \frac{\sin\left[\left(M + \frac{1}{2}\right)ks_x u(\theta, \phi)\right]}{\sin\left[\frac{1}{2}ks_x u(\theta, \phi)\right]} \right\} \left\{ \frac{\sin\left[\left(N + \frac{1}{2}\right)ks_y v(\theta, \phi)\right]}{\sin\left[\frac{1}{2}ks_y v(\theta, \phi)\right]} \right\} \\ - \alpha \left\{ \frac{\sin\left[\left(M + \frac{1}{2}\right)ks_x u(\theta, \phi)\right]}{\sin\left[\frac{1}{2}ks_x u(\theta_s, \phi_s)\right]} \right\} \left\{ \frac{\sin\left[\left(N + \frac{1}{2}\right)ks_y v(\theta, \phi)\right]}{\sin\left[\frac{1}{2}ks_y v(\theta_s, \phi_s)\right]} \right\} \\ - \beta \left\{ \frac{\sin\left[\left(M + \frac{1}{2}\right)ks_x u(\theta, \phi)\right]}{\sin\left[\frac{1}{2}ks_x u(\theta, \phi)\right]} \right\} \left\{ \frac{\sin\left[\left(N + \frac{1}{2}\right)ks_y v(\theta, \phi)\right]}{\sin\left[\frac{1}{2}ks_y v(\theta_s, \phi_s)\right]} \right\}$$

The resulting total far zone field is as indicated here.



Suppression Contours

$$\alpha \left\{ \frac{\sin\left[\frac{1}{2} k s_x u(\theta, \phi)\right]}{\sin\left[\frac{1}{2} k s_x u(\theta_S, \phi_S)\right]} \right\} + (1 - \alpha) \left\{ \frac{\sin\left[\frac{1}{2} k s_y v(\theta, \phi)\right]}{\sin\left[\frac{1}{2} k s_y v(\theta_S, \phi_S)\right]} \right\} = 1$$

The sidelobe suppression will occur along contours satisfying this equation. Obviously, these contours pass through the point (θ_S, ϕ_S) .



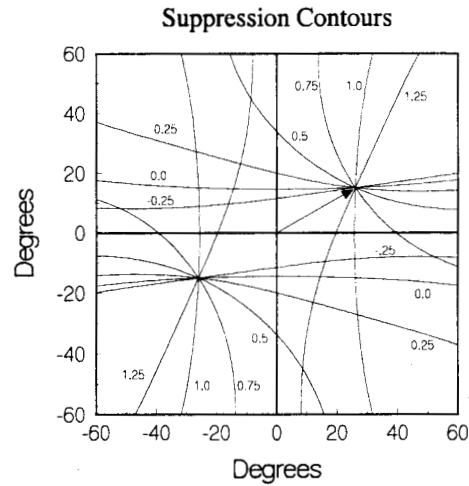
Angular Coordinate System

$$\theta_x = \theta \cos \phi$$

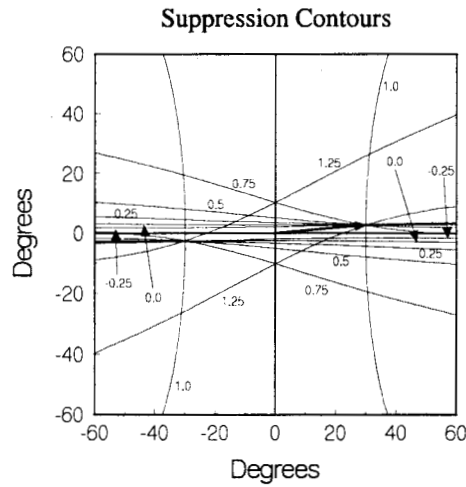
$$\theta_y = \theta \sin \phi$$

In plotting the far zone patterns a coordinate system will be used which treats the polar angular coordinates as Cartesian variables. This introduces some distortion of the pattern compared with the more familiar (u,v) system but has the advantage of more faithful representation of the lobe widths at the extremes of the angular range.

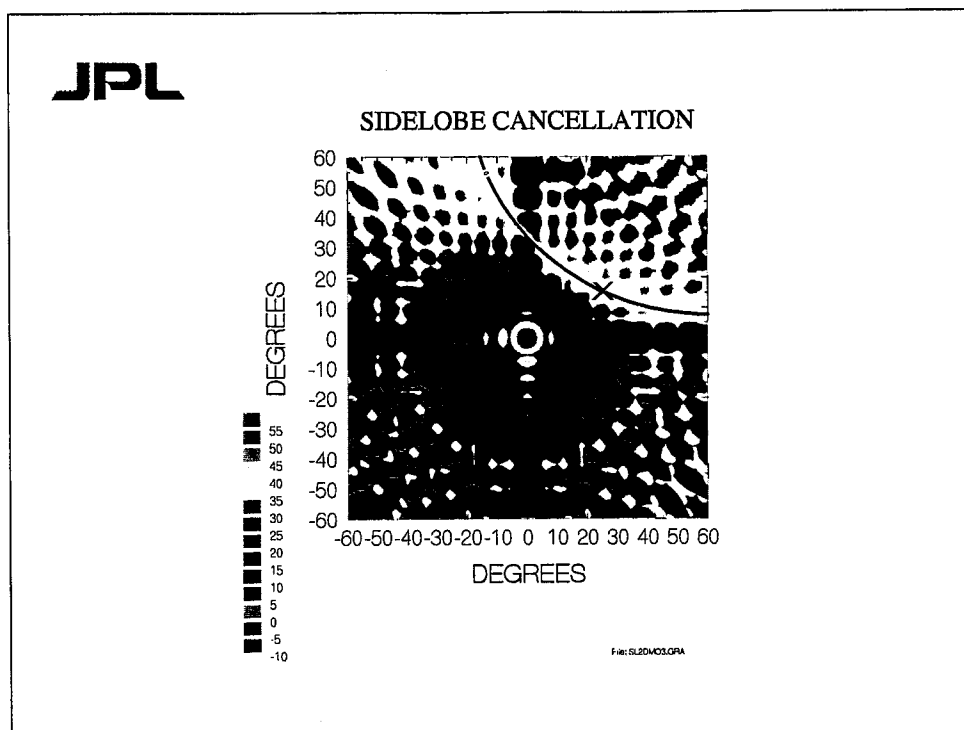
JPL



As α varies, the curve rotates around (θ_s, ϕ_s) as shown here for the case when $\theta_s = 30^\circ$ and $\phi_s = 30^\circ$. The arrow indicates the location of the point (θ_s, ϕ_s) . The curves passing through the point $(30^\circ, 210^\circ)$ are accessible by reversing the sign of the perimeter excitations relative to the original array. For large values of α (positive or negative) the limiting curves pass through both $(30^\circ, 30^\circ)$ and $(30^\circ, 210^\circ)$. From the definition of u and v one can easily see that scanning the main beam merely produces a shift in the u, v plane. Thus, it is clear that under scanning the two intersection points move in a manner similar to the motion of the beam. Therefore, by varying θ_s , ϕ_s , and α , one may position the suppression region to cover any two desired points in the hemisphere and, of course, the rest of the points along the corresponding curve defined by (20). The suppression described by Kott is recovered by setting α equal to 0 for a horizontal null or 1 for a vertical null.



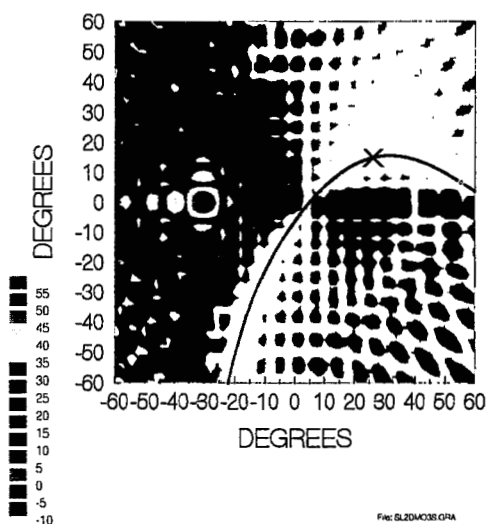
This graph shows the effect of moving the suppression region position (θ_s, ϕ_s) closer to the x-axis. Note that all of the contours except the two for $\alpha=1$ move toward horizontal. In fact, if (θ_s, ϕ_s) is placed on the x-axis, all of the contours except those for $\alpha=1$ become horizontal, coincide, and pass through the main beam. In general, this will occur whenever the line between (θ_B, ϕ_B) and (θ_s, ϕ_s) is horizontal and a similar phenomenon occurs when this line is vertical.



Four examples are presented to illustrate the independent nature of the steering of the main beam and the suppression region in two dimensions. A 21×21 element array with half wavelength element spacing is considered. Four 21 element linear arrays are added one-quarter wavelength from each edge. The first example far zone field, shown here, illustrates the case in which the main beam is unscanned and the suppression region is set to pass through $(\theta_s, \phi_s) = (30^\circ, 30^\circ)$ and placing the suppression region primarily in the first quadrant. The corresponding curve from Figure 10a is superimposed on the plot indicating that the suppression region follows the expected trajectory and the "X" locates (θ_s, ϕ_s) .

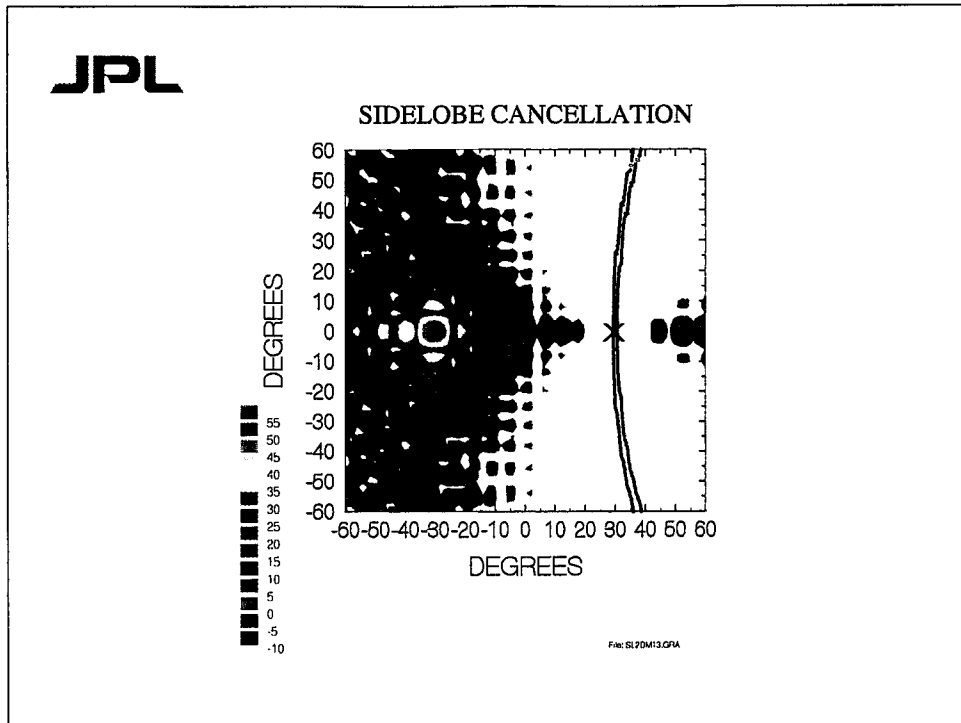
JPL

SIDELobe CANCELLATION



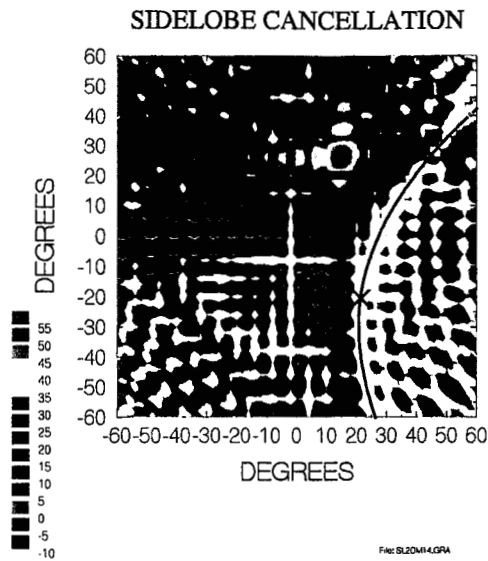
File: GL2DA038.GRA

The second example, shown here, illustrates a case in which the main beam is scanned to $(\theta_B, \phi_B) = (30^\circ, 180^\circ)$ while the suppression region is centered at $(\theta_S, \phi_S) = (30^\circ, 30^\circ)$ and . Here, again, the expected trajectory from (20) is superimposed and "X" locates (θ_S, ϕ_S) .



Similarly, the third example, shown in this graph, illustrates a case in which the main beam is scanned to $(\theta_B, \phi_B) = (30^\circ, 180^\circ)$ while the suppression region is centered at $(\theta_S, \phi_S) = (30^\circ, 0^\circ)$. For this case α *must* be unity because Q becomes infinite. This is a case of the sort discussed previously by Kott.

JPL



Finally, this graph illustrates a more general case in which the main beam is scanned to $(\theta_B, \phi_B) = (30^\circ, 60^\circ)$ while the suppression region is centered at $(\theta_S, \phi_S) = (30^\circ, -45^\circ)$ and . These examples indicate the overall performance achieved with this two dimensional generalization of the Kott scheme.



Concluding Summary

- Uniform illumination is optimum for Kott's sidelobe suppression technique.
- For uniform illumination an optimum position exists for the added elements.
- Generalization to two-dimensional arrays leads to suppression contours.
- Coupled oscillator phase control easily implements Kott sidelobe suppression.

It has been shown that, under the assumption of uniform aperture illumination, the sidelobe suppression concept due to Kott can be conveniently and optimally implemented in an array using the coupled oscillator aperture phase control scheme of Liao and York. Moreover, the two-dimensional generalization of the coupled oscillator scheme has been shown to provide for a two-dimensional generalization of the Kott scheme resulting in a two-dimensional array with independently steerable main beam and sidelobe suppression region.